Turk J Elec Engin, VOL.10, NO.3 2002, © TÜBİTAK

Stability Analysis of a Closed-Loop Control for a Pulse Width Modulated DC Motor Drive

Fatma GÜRBÜZ, Eyüp AKPINAR
Dokuz Eylül University, Department of Electrical and Electronics Engineering,
Tınaztepe, Buca, 35160 İzmir-TURKEY
e-mail: fatma.gurbuz@eee.deu.edu.tr

Abstract

In this paper, the effect of the variation of amplitude and the chopping period of a PWM signal on the stability of a closed-loop control for a DC motor drive is investigated. First, the entire system is formulated as a Linear Quadratic (LQ) tracker with output feedback [1]. Then, stability analysis for the varying amplitude and the varying chopping period is carried out by the methods of root locus and the Jury test. Finally, stability limits obtained from a root locus and Jury test are checked by the simulation of the system in MATLAB.

Key Words: *pulse width modulation (PWM), DC drive, stability analysis.*

1. Introduction

Digital electronics are widely used in motor control. These controllers are more accurate, flexible in terms of software and less expensive following the rapid development in integrated circuit technology. In addition protection functions for the reliable operation of drive circuits are easily implemented in digital controllers. While the controllers are digital, the motors are analog and, therefore, signals between the controller and motor are linked to each other using analog to digital converters. Control system design techniques are usually implemented on electrical machines and drives by using continuous time system models, and the drives are modeled by average representation. Therefore, switching-frequency components are eliminated and are not included in the models. When the discrete time system model is established for a motor drive, the effect of switching frequency can be taken into account. In this paper, the machine, drive and controller are modeled in z-domain in order to investigate the effect of switching the frequency of the chopper drive on stability.

A separately excited DC motor is considered to be a multi-input, multi-output system. This machine is widely used in many variable speed drives. Open-loop operation of the motor can be unsatisfactory in some industrial applications. If the drive requires constant-speed operation under changing load torque, closed-loop control is necessary. The closed-loop speed control system in this study consists of a separately excited DC motor, a class C pulse width modulated (PWM) chopper, and proportional integral type (PI) speed and current controllers. The block diagram representation of the system is given in Figure 1. The closed-loop control of the motor has basically two feedback loops. The outer loop is a speed feedback loop

and the inner loop is the current feedback loop. The controllers used in these loops are both of PI type. The speed controller output is the reference for the current controller. The output of the current controller is the input to the pulse width modulated (PWM) generator that controls the motor input voltage [2]. Although the DC machine can be modeled in a continuous time domain, when PWM techniques based on digital controllers are used, discrete-time domain modeling enables the identification of instability regions of the entire system as a function of switching frequency.

The stability analysis of discrete-time systems can be carried out using two different techniques. One of them is direct stability analysis in z-domain such as the Jury test, and the Schur-Cohn criterion. The other covers the techniques used for continuous-time systems after certain modifications are made. The latter includes the Routh-Hurwitz criterion, root-locus method and frequency-response techniques.

In this study, the stability analysis of closed-loop system under variation of chopping periods, T, and amplitude of PWM waveforms, K_{pwm}, is carried out using the LQ tracker model. The characteristic equation of the system can be obtained as a linear function of K_{pwm}. However, the characteristic equation cannot be obtained as a linear function of T. Thus, the stability analysis of the system for the amplitude of PWM signal is investigated by both rootlocus and the Jury test though it is done by only the Jury test for the variable chopping period.

2. Modeling of the Closed-Loop System

A separately excited DC machine whose field current is kept constant can be described in continuous time by the state space form as follows [3].

$$\frac{d}{dt}\begin{bmatrix} i_a(t) \\ w(t) \end{bmatrix} = \begin{bmatrix} -R_a/L_a & -K_a\varphi/L_a \\ K_a\varphi/J & -B_v/J \end{bmatrix} \cdot \begin{bmatrix} i_a(t) \\ w(t) \end{bmatrix} + \begin{bmatrix} 1/L_a & 0 \\ 0 & -1/J \end{bmatrix} \cdot \begin{bmatrix} V_a(t) \\ T_L(t) \end{bmatrix} \tag{1}$$

or in the compact form

$$\frac{d}{dt}x_m(t) = A_m \cdot x_m(t) + B_m \cdot u_m(t) \tag{2}$$

where R_a is armature resistance (Ohm), L_a is armature inductance (Henry), $K_a\varphi$ is back electromotive force and torque constant (Volt/rd/sec or Nt-m/Ampere), J is total moment of inertia (kg-m^2) and B_v is viscous friction constant (Nt-m/rd/sec). The armature current and rotor speed are chosen as state variables. The armature voltage and load torque can be considered as input variables.

The variable $V_a(t)$ in Equation (1) represents the amplitude of the voltage applied to the armature by the chopper circuit. A class-C type of chopper given in Figure 2 is used. This voltage is a function of t_{on} and the amplitude of the voltage K_{pwm}, as shown in Figure 3. Since the amplitude of voltage is kept constant, t_{on} will be taken into account as the input variable in the motor model given in Equation (1) instead of $V_a(t)$.

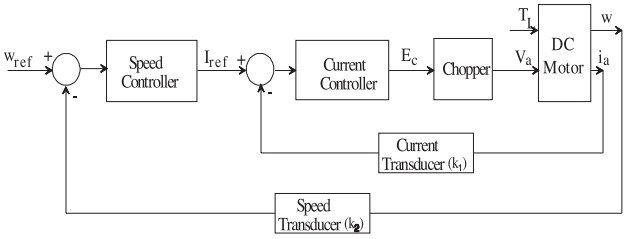

Figure 1. Block diagram of the DC motor speed control system

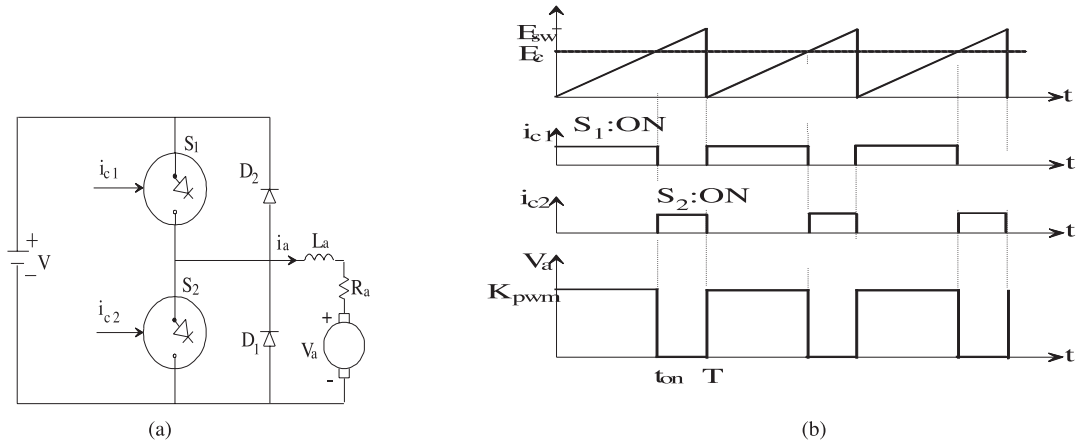

Figure 2. (a) Class-C chopper circuit and (b) related waveform

In order to describe the PWM waveform in the model, the entire system is modeled in z-domain. Under the assumption that the sampling period (T) is much smaller than the time constant of the system, which is a practical assumption, the state-space model of the PWM driven DC motor can be written as given in the following equation for the motor if a single input (such as t_{on}) is considered [4]

$$x_m[(n+1)\,T] = \{I + A_m T\} x_m(nT) + K_{pwm} b t_{on}(nT) \tag{3}$$

When the load torque is taken as the other input for the motor, the state-space model of the PWM driven DC motor can be obtained as [5]

$$x_m[(n+1)T] = [I + A_m T] x_m(nT) + \begin{bmatrix} K_{pwm}/L_a & 0 \\ 0 & -T/J \end{bmatrix} \begin{bmatrix} t_{on}(nT) \\ T_L \end{bmatrix} \tag{4}$$

By substituting the variables of Equation (1) into (4), and dropping T, the discrete-time state equation of the DC motor driven by a class C chopper is obtained as [5]

$$\begin{bmatrix} i_a \\ w \end{bmatrix}_{n+1} = \begin{bmatrix} (L_a - R_a)/L_a & -K_a \varphi T/L_a \\ K_a \varphi T/J & (J - B_v T)/J \end{bmatrix} \cdot \begin{bmatrix} i_a \\ w \end{bmatrix}_n + \begin{bmatrix} K_{pwm}/L_a & 0 \\ 0 & -T/J \end{bmatrix} \cdot \begin{bmatrix} t_{on} \\ T_L \end{bmatrix}_n \tag{5}$$

In this study, the transfer functions of both current and speed controller are obtained by using the trapezoidal integration rule. The basic advantage of the trapezoidal integration rule is that the entire left half s-plane maps to the interior of the unit circle in the z-plane; thus all stable analog systems will result

in stable digital ones [6]. A digital PI controller transfer function using the trapezoidal integration rule is given in the form of

$$K_p + K_i \frac{T}{2} \frac{(z+1)}{(z-1)} \tag{6}$$

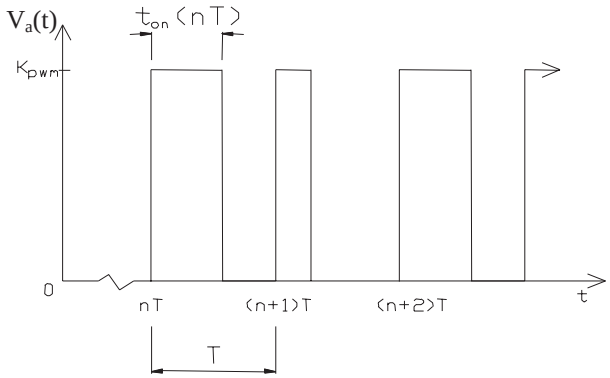

Figure 3. Pulse width modulated signal

where K_p is the proportional constant, K_i is the integral constant, and the T is the sampling period. Since sampling the PWM waveform once in a period is sufficient, the sampling period is taken as the same with chopping period for simplicity in analysis. In this work, a unit delay term is used to include all the computational and loop delays that may occur, thus transfer function of the current controller, $G_{ci}(z)$, is taken as

$$G_{ci}(z) = \frac{K_{pi}}{z} + \frac{K_{ii}}{z} \frac{T}{2} \frac{(z+1)}{(z-1)} \tag{7}$$

where K_{pi} is the proportional constant and K_{ii} is the integral constant of the current controller. A block diagram representation of this transfer function is depicted in Figure 4.

The state-space model of the current controller is given below

$$\begin{bmatrix} \varepsilon_{1i} \\ \varepsilon_{2i} \end{bmatrix}_{n+1} = \begin{bmatrix} 0 & 0 \\ T/2 & 1 \end{bmatrix} \cdot \begin{bmatrix} \varepsilon_{1i} \\ \varepsilon_{2i} \end{bmatrix}_n + \begin{bmatrix} 1 & -k_1 \\ \frac{T}{2} & -k_1 \cdot \frac{T}{2} \end{bmatrix} \cdot \begin{bmatrix} I_{ref} \\ i_a \end{bmatrix}_n \tag{8}$$

and the output variable is

$$E_c(n) = \begin{bmatrix} K_{pi} & K_{ii} \end{bmatrix} \cdot \begin{bmatrix} \varepsilon_{1i} \\ \varepsilon_{2i} \end{bmatrix}_n \tag{9}$$

Similar to that of the current controller, the speed controller transfer function, $G_{cs}(z)$, is taken as

$$G_{cs}(z) = \frac{K_{ps}}{z} + \frac{K_{is}}{z} \frac{T}{2} \frac{(z+1)}{(z-1)} \tag{10}$$

where K_{ps} is the proportional constant and K_{is} is the integral constant of the speed controller. Block diagram representation of this transfer function is depicted in Figure 5.

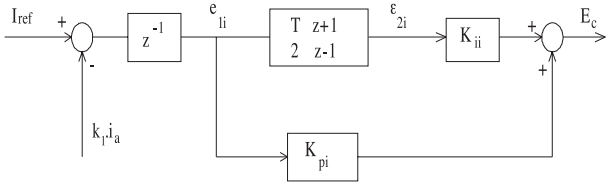

Figure 4. Block diagram of the current controller

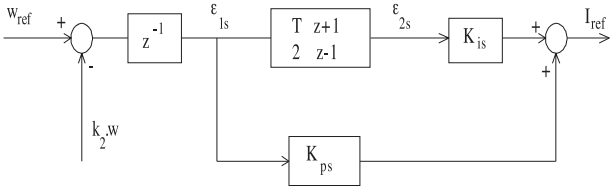

Figure 5. Block diagram of the speed controller

The state-space model of the speed controller is as given below

$$\begin{bmatrix} \varepsilon_{1s} \\ \varepsilon_{2s} \end{bmatrix}_{n+1} = \begin{bmatrix} 0 & 0 \\ T/2 & 1 \end{bmatrix} \cdot \begin{bmatrix} \varepsilon_{1s} \\ \varepsilon_{2s} \end{bmatrix}_n + \begin{bmatrix} 1 & -k_2 \\ \frac{T}{2} & -k_2 \cdot \frac{T}{2} \end{bmatrix} \cdot \begin{bmatrix} \omega_{ref} \\ \omega \end{bmatrix}_n \tag{11}$$

and the output equation is

$$I_{ref}(n) = \begin{bmatrix} K_{ps} & K_{is} \end{bmatrix} \cdot \begin{bmatrix} \varepsilon_{1s} \\ \varepsilon_{2s} \end{bmatrix}_n \tag{12}$$

If the model of each subsystem given above is examined, it is observed that the entire system has 6 state variables. These are i_a, ω, ε_{1i}, ε_{2i}, ε_{1s}, and ε_{2s}. This closed loop system has two external inputs, which are ω_{ref} and T_L. Therefore, by linking the internal variables between the models of subsystems, the state-space form of the entire system can be developed in terms of state variables and external inputs as [7]

$$\begin{aligned} \begin{bmatrix} i_a \\ \omega \\ \varepsilon_{1i} \\ \varepsilon_{2i} \\ \varepsilon_{1s} \\ \varepsilon_{2s} \end{bmatrix}_{n+1} &= \begin{bmatrix} (L_a - R_a T)/L_a & -K_a \varphi T/L_a & 0 & 0 & 0 & 0 \\ K_a \varphi T/J & (J - B_v T)/J & 0 & 0 & 0 & 0 \\ -k_1 & 0 & 0 & 0 & 0 & 0 \\ -k_1 \cdot T/2 & 0 & T/2 & 1 & 0 & 0 \\ 0 & -k_2 & 0 & 0 & 0 & 0 \\ 0 & -k_2 \cdot T/2 & 0 & 0 & T/2 & 1 \end{bmatrix} \cdot \begin{bmatrix} i_a \\ \omega \\ \varepsilon_{1i} \\ \varepsilon_{2i} \\ \varepsilon_{1s} \\ \varepsilon_{2s} \end{bmatrix}_n \\ &+ \begin{bmatrix} 0 & \frac{K_{pwm}}{L_a}\frac{T}{E_{sw}} \\ 0 & 0 \\ 1 & 0 \\ T/2 & 0 \\ 0 & 0 \\ 0 & 0 \end{bmatrix} \cdot \begin{bmatrix} I_{ref} \\ E_c \end{bmatrix}_n + \begin{bmatrix} 0 & 0 \\ 0 & -T/J \\ 0 & 0 \\ 0 & 0 \\ 1 & 0 \\ T/2 & 0 \end{bmatrix} \cdot \begin{bmatrix} \omega_{ref} \\ T_L \end{bmatrix}_n \end{aligned} \tag{13}$$

or, in compact form

$$x(n+1) = Ax(n) + Bu(n) + Er(n) \tag{14}$$

Since the control law for the output feedback is of the form [8]

$$u(n) = -Ky(n) \tag{15}$$

the linear gains that are the relation between $u(n)$ and $y(n)$ can be obtained from Equation (9) and Equation (12) as follows:

$$\begin{bmatrix} I_{ref} \\ E_c \end{bmatrix}_n = -\begin{bmatrix} 0 & 0 & -K_{ps} & -K_{is} \\ -K_{pi} & -K_{ii} & 0 & 0 \end{bmatrix} \cdot \begin{bmatrix} \varepsilon_{1i} \\ \varepsilon_{2i} \\ \varepsilon_{1s} \\ \varepsilon_{2s} \end{bmatrix}_n \tag{16}$$

where

$$K = \begin{bmatrix} 0 & 0 & -K_{ps} & -K_{is} \\ -K_{pi} & -K_{ii} & 0 & 0 \end{bmatrix} \tag{17}$$

and

$$y = \begin{bmatrix} \varepsilon_{1i} & \varepsilon_{2i} & \varepsilon_{1s} & \varepsilon_{2s} \end{bmatrix}^T \tag{18}$$

The output vector can be written in terms of the state vector as given below

$$y(n) = C.x(n) \tag{19}$$

where

$$C = \begin{bmatrix} 0 & 0 & 1 & 0 & 0 & 0 \\ 0 & 0 & 0 & 1 & 0 & 0 \\ 0 & 0 & 0 & 0 & 1 & 0 \\ 0 & 0 & 0 & 0 & 0 & 1 \end{bmatrix}. \tag{20}$$

Thus, the entire system model defined in Equation (14) can also be written as

$$x(n+1) = [A - BKC]x(n) + Er(n) \tag{21}$$

A block diagram representation of the LQ tracker model of the system with output feedback is shown in Figure 6.

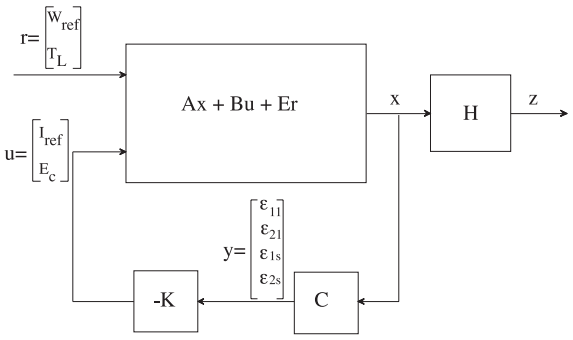

Figure 6. Block diagram representation of the system as an LQ tracker with output feedback

3. Stability Analysis

A number of methods of analyzing power electronics circuits applied on electrical machines are discussed in [9]. A DC motor drive controlled by PWM technique can be analyzed either by neglecting all harmonics produced by the chopper circuit, retaining only the average value in the Fourier series expansion of output waveform, or analyzing the low frequency, small-signal response of switching circuits. The small signal model makes the application of Laplace transforms, state variables and small displacement theory possible. The steady state duty ratio can be included in this mode. This small-signal model enables the disturbances around the steady state operating point. The stability analysis of the system given in Equation (21) can be carried out under large signal perturbations by using the z-domain technique and sampling the PWM waveform as a function of its magnitude and period.

The characteristic equation of the system given in Equation (21) is

$$\det(zI - (A - BKC)) = 0 \tag{22}$$

where I is the identity matrix, and the matrices A, B, K and C have been given in Equations (13), (17), and (20).

In this study, 110V, 2.5 hp, 1800 rpm separately excited DC motor having the following parameters is used: R_a=1 ohm, L_a=46 mH, J=0.093 kgm^2, B_v=0.008 Nt-m/rd/sec, $K_a\varphi$=0.55 V/rad/sec. The other parameters related to the system are given below.

Sampling period, T=0.0001 sec,

Amplitude of PWM signal, K_{pwm}=110 V

Peak value of the sawtooth waveform, E_{sw}=12 V

Reference speed, w_{ref}=80 rad/sec

Load torque, T_L=0

Controller parameters used in this study are as follows: K_{pi}=10, K_{ps}=1, K_{is}=5, K_{ii}=500. In addition, the linear gains of current and speed transducers (k_1 and k_2) have been chosen as unity.

3.1. The Amplitude Control of PWM

The structure of characteristic equation as a function of the amplitude of PWM waveform enables the application of both root-locus and the Jury test on the stability of the system. The characteristic equation as a function of the amplitude of a PWM signal K_{pwm} has been obtained by a dedicated program written in MATHCAD [10], as given below.

$$\begin{aligned} &z^6 - 3.99781748481z^5 + 5.99345318022z^4 - 3.99345390603z^3 + 0.997818210612z^2 \\ &+K_{pwm}(1.81612318841 \cdot 10^{-3}z^4 - 5.43929597164 \cdot 10^{-3}z^3 + 5.43129677584 \cdot 10^{-3}z^2 \\ &-1.80919241724 \cdot 10^{-3}z + 1.06842730978 \cdot 10^{-6}) \end{aligned} \tag{23}$$

This equation is rearranged as follows in order to get it in the suitable form for root locus analysis.

$$1 + K_{pwm}\frac{num(z)}{den(z)} = 0 \tag{24}$$

The root-locus technique on the stability of system is applied as the K_{pwm} is taken into account as a varying parameter. The values of K_{pwm} and corresponding root locations are obtained with the aid of the rlocus function available in the MATLAB Control System Toolbox [11]. By examining the list of root location and expanding the regions around the unit circle, it is seen that for stable operation K_{pwm} must be kept in the range

$$3.0 < K_{pwm} < 550.$$

Analysis of the system is performed in MATLAB [12]. The analysis results of the system for K_{pwm}=545 in stable region and K_{pwm}=555 in the unstable region are presented in Figures 7-10. Figures 7 and 8 give the speed and current response, respectively, for the amplitude value of 545 of PWM signal. In these figures both the speed and current responses settle down and this confirms the stable operation for that value of K_{pwm}.

Figures 9 and 10 show the speed and current responses, respectively, for the PWM amplitude value at 555. As seen from these figures, both the speed and current responses are increasing in time and this shows the unstable operation.

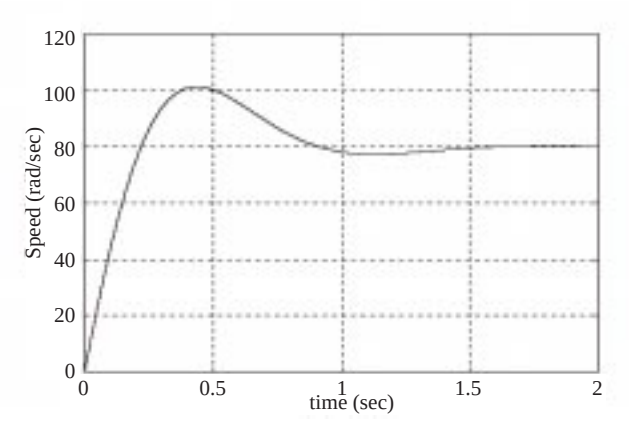

Figure 7. Rotor speed for K_{pwm}=545

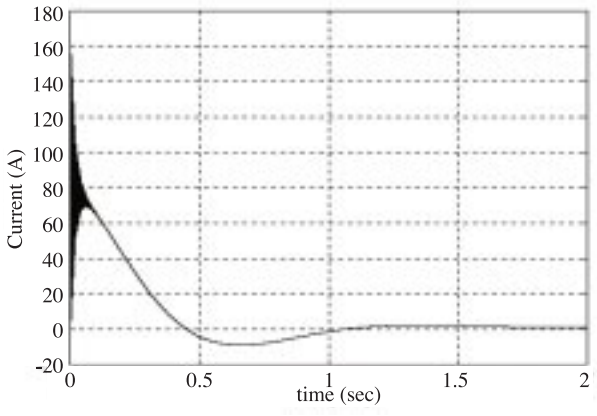

Figure 8. Armature current for K_{pwm}=545

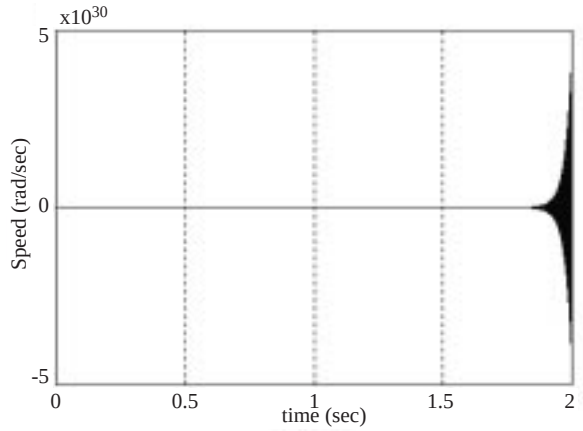

Figure 9. Rotor speed for K_{pwm}=555

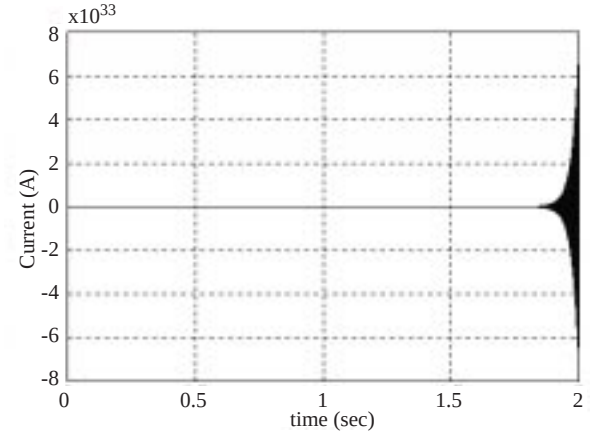

Figure 10. Armature current for K_{pwm}=555

The Jury test is also applied to the characteristic equation written as a function of z. Since the system is sixth order, the characteristic equation of the system can be obtained in the form of

$$Q(z) = a_6 z^6 + a_5 z^5 + a_4 z^4 + a_3 z^3 + a_2 z^2 + a_1 z^1 + a_0 = 0 \tag{25}$$

where $a_6 > 0$. Then the Table 1 given below is created.

Table 1. Jury table for the 6^{th} order system in this study

z^0	z^1	z^2	z^3	z^4	z^5	z^6
a_0	a_1	a_2	a_3	a_4	a_5	a_6
a_6	a_5	a_4	a_3	a_2	a_1	a_0
b_0	b_1	b_2	b_3	b_4	b_5	
b_5	b_4	b_3	b_2	b_1	b_0	
c_0	c_1	c_2	c_3	c_4		
c_4	c_3	c_2	c_1	c_0		
d_0	d_1	d_2	d_3			
d_3	d_2	d_1	d_0			
e_0	e_1	e_2				

where

$$b_k = \begin{vmatrix} a_0 & a_{6-k} \\ a_6 & a_k \end{vmatrix}, \tag{26}$$

$$c_k = \begin{vmatrix} b_0 & b_{5-k} \\ b_5 & b_k \end{vmatrix}, \tag{27}$$

$$d_k = \begin{vmatrix} c_0 & c_{4-k} \\ c_4 & c_k \end{vmatrix}, \tag{28}$$

$$e_k = \begin{vmatrix} d_0 & d_{3-k} \\ d_3 & d_k \end{vmatrix}, \tag{29}$$

According to the Jury test, the following conditions must be satisfied for stability [6]

$$Q(1) > 0 \tag{30}$$

$$(-1)^6 Q(-1) > 0 \tag{31}$$

$$|a_0| < a_6 \tag{32}$$

$$|b_0| > |b_5| \tag{33}$$

$$|c_0| > |c_4| \tag{34}$$

$$|d_0| > |d_3| \tag{35}$$

$$|e_0| > |e_2| \tag{36}$$

After rearranging the characteristic equation given in (23) into the form of (25), the coefficients of (25) can be obtained as

$a_o = 1.06842730978.10^{-6}K_{pwm}$
$a_1 = 1.80919241724.10^{-3}K_{pwm}$
$a_2 = 0.997818210612 + 5.43129677584.10^{-3}K_{pwm}$
$a_3 = -3.99345390603 - 5.43929597164.10^{-3}K_{pwm}$
$a_4 = 5.99345318022 + 1.81612318841.10^{-3}K_{pwm}$
$a_5 = -3.99781748481$
$a_6 = 1$

Using these values in Table 1, the coefficients b_k, c_k, d_k and e_k in (26)-(29) are obtained using MATHCAD. Since these coefficients hold too much space, they are not given here. They are given in [5].

By solving the stability constraints given in (30)-(36), the stable region of system as a function of K_{pwm} is obtained as follows;

$$2.9853 < K_{pwm} < 549.7.$$

The results of the Jury stability test are consistent with the results of the stability analysis obtained from the root-locus method.

3.2. Chopping Period Control

The chopping period T is kept as variable in the characteristic equation. Then, the characteristic equation is obtained as given in Equation (37)

$$Q(z) = a_6z^6 + a_5z^5 + a_4z^4 + a_3z^3 + a_2z^2 + a_1z^1 + a_0 \tag{37}$$

where

$a_0 = -324090.307T^3 + 11785.102T^2 + 736568.879T^4$
$a_1 = -1992.75362T + 1473137.76T^4 + 26420.0562T^2 - 4285.49167T^3$
$a_2 = 1 + 5956.43571T + 736568.879T^4 + 324090.307T^3 - 38303.9972T^2$
$a_3 = -4 - 5912.7854T - 49792.5822T^2 + 4285.49167T^3$
$a_4 = 6 + 1927.27816T + 49891.4212T^2$
$a_5 = -4 + 21.8251519T$
$a_6 = 1$

As can be clearly observed from (37), the characteristic equation of the system is not in the proper form for the stability analysis to be carried out by the root-locus technique. Therefore the stability analysis for the varying chopping period is investigated by the Jury test method. By solving the stability constraints given in (30)-(36), the interval of chopping period T for the stable region of the system is obtained as follows,

$$0 < T < 0.0004969$$

As a consequence, the chopping frequency must be kept in the range

$$2012.47Hz < f < \infty\infty$$

The system has been analyzed for the frequency of 2010 Hz and 2020 Hz. One of them is in the stable and the other is in the unstable region. Figure 11 and 12 give the speed and current responses respectively for the chopping frequency of 2010 Hz. As it is seen from these figures, both the speed and current responses are increasing in time, and this shows the instability. Figures 13 and 14 show the speed and current responses for the chopping frequency of 2020 Hz. In these figures both the speed and current response settle down and this denotes the stable operation for 2020 Hz.

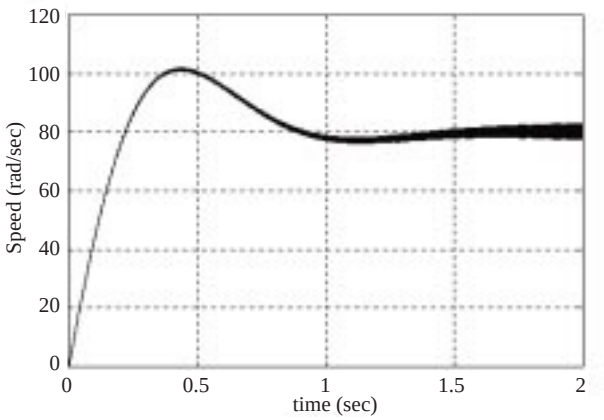

Figure 11. Speed of the motor showing instability

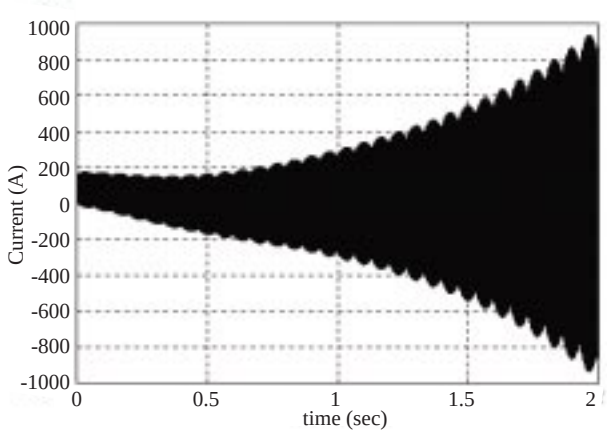

Figure 12. Armature current showing instability

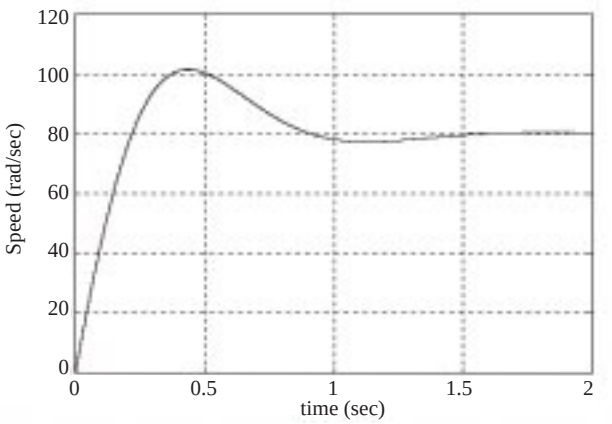

Figure 13. Speed of the motor showing stability

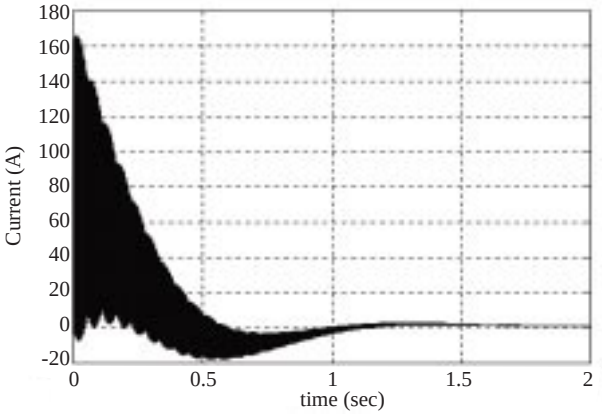

Figure 14. Armature current showing stability

4. Conclusions

A separately excited DC motor controlled by the cascade current and speed controllers is modeled in difference equations. Therefore, all the harmonics of the PWM waveform are covered by the model and the model is brought into the linear quadratic tracker form with output feedback.

The region of stable operation of the closed-loop system has been identified for various chopping periods and amplitudes of PWM input voltage to the armature of a separately excited DC motor. It was found that there is an unstable region for some values of these two variables. This region depends on the moment of inertia, damping coefficient, and the other parameters of the motor as well as the PI parameters.

References

[1] F. L. Lewis, *Applied Optimal Control & Estimation Digital Design & Impementation*, Prentice-Hall,. 1992.

[2] P. C. Sen, *Thyristor DC Drives*, John Wiley and Sons, 1991(reprint ed.)

[3] P. C. Krause, O. Wasynczuk, S. D. Sudhoff, '*Analysis of Electric Machinery*', IEEE Press, 1994.

[4] P. F. Muir, & C. P. Neuman, "Pulsewidth Modulation Control of Brushless DC Motors for Robotic Applications" *IEEE Transactions on Industrial Electronics*, vol. IE-32, n.3, 1985, pp.222-229.

[5] F. Gürbüz, *Optimal Control of Digitally Controlled DC Motors,* Ph.D. Thesis, Dokuz Eylül University, İzmir, 1997.

[6] C. L. Phillips, & H. T. Nagle, *Digital Control System Analysis and Design,* Prentice-Hall, 1984.

[7] F. Gürbüz, E. Akpinar, "Optimal Control of Digitally Controlled DC Drive Using a Quadratic Performance Index", *Proceedings of the 1998 International Conference on Electrical Machines (ICEM'98),* pp.1207-1212.

[8] L. Umanand, & S. R. Bhat, "Optimal and robust digital current controller synthesis for vector-controlled induction motor drive systems", *IEE Proc. Electr. Power Appl.* vol. 143, n. 2, 1996, pp. 141-150.

[9] R. G. Hoft, J. B. Casteel, "Power Electronic Circuit Analysis Techniques", lecture notes, University of Missouri-Columbia, USA.

[10] The MathSoft Inc, *MATHCAD User's Guide (4^{th} printing),* 1993.

[11] The MathWorks Inc, *MATLAB Control System Toolbox ver 3.0b,* 1993.

[12] The MathWorks Inc, *MATLAB High Performance Numeric Computation and Visualization Software User's Guide*, 1993.